Mon. Not. R. Astron. Soc. **395,** 1087–1091 (2009) doi:10.1111/j.1365-2966.2009.14605.x

Ultraviolet Fe II emission in $z \sim 2$ quasars

H. Sameshima,[1★] J. Maza,[2] Y. Matsuoka,[1] S. Oyabu,[3] K. Kawara,[1] Y. Yoshii,[1] N. Asami,[1] N. Ienaka[1] and Y. Tsuzuki[4]

[1] *Institute of Astronomy, University of Tokyo, 2-21-1, Osawa, Mitaka, Tokyo 181-0015, Japan*
[2] *Departamento de Astronomia, Universidad de Chile, Casilla 36-D, Santiago, Chile*
[3] *Institute of Space and Astronautical Science, Japan Aerospace Exploration Agency, Kanagawa 229-8510, Japan*
[4] *System Integration Service Department, Redfox Inc., 3-3-11, Kita-Aoyama, Minato-ku, Tokyo 107-0061, Japan*

Accepted 2009 February 5. Received 2009 January 17

ABSTRACT

We present spectra of six luminous quasars at $z \sim 2$, covering rest wavelengths 1600−3200 Å. The fluxes of the UV Fe II emission lines and Mg II λ2798 doublet, the line widths of Mg II and the 3000 Å luminosity were obtained from the spectra. These quantities were compared with those of low-redshift quasars at $z = 0.06$–0.55 studied by Tsuzuki et al. In a plot of the Fe II(UV)/Mg II flux ratio as a function of the central black hole mass, Fe II(UV)/Mg II in our $z \sim 2$ quasars is systematically greater than in the low-redshift quasars. We confirmed that luminosity is not responsible for this excess. It is unclear whether this excess is caused by rich Fe abundance at $z \sim 2$ over low-redshift or by non-abundance effects such as high gas density, strong radiation field and high microturbulent velocity.

Key words: galaxies: abundances – galaxies: active – line: formation – quasars: emission lines.

1 INTRODUCTION

According to the models of explosive nucleosynthesis, much of the iron comes from Type Ia supernovae, while α elements such as O and Mg come from Type II supernovae. Because of the difference in lifetime of the progenitors, it is generally considered that the iron enrichment delays relative to α elements by 1–2 billion years (Hamann & Ferland 1993; Yoshii, Tsujimoto & Nomoto 1996; Yoshii, Tsujimoto & Kawara 1998). If Fe II/Mg II, the relative strengths of Fe II emission lines and the Mg II λ2798 doublet, reflects the Fe/Mg abundance ratio, there will be a break in Fe II/Mg II at high redshift. Despite much efforts made by many observational groups (e.g. Elston, Thompson & Hill 1994; Kawara et al. 1996; Dietrich et al. 2002, 2003; Iwamuro et al. 2002, 2004; Freudling, Corbin & Korista 2003; Maiolino et al. 2003; Tsuzuki et al. 2006; Kurk et al. 2007; Matsuoka et al. 2007; Matsuoka, Kawara & Oyabu 2008), there have been found no signs of such a break; Fe II/Mg II looks constant from low-redshift up to $z \sim 6.5$ with large scatter.

No break in Fe II/Mg II might reflect a significantly shorter delay-time of 0.2–0.6 Gyr, as suggested by Friaça & Terlevich (1998), Matteucci & Recchi (2001) and Granato et al. (2004). The expected break can also be obscured by non-abundance effects. Simulations of Fe II emitting regions, assuming either photoionization or shocks, imply that the Fe abundance is not the only parameter which controls the Fe II strength, but several non-abundance factors can also affect it. Such non-abundance factors include spectral energy distribution (SED) of the central source, strength of the radiation field and the gas density of broad emission line region (BELR) clouds. Recently, Verner et al. (2003) and Baldwin et al. (2004) pointed out that a large microturbulence velocity might be responsible for strong Fe II emission. Tsuzuki et al. (2006) have studied non-abundance factors by using spectra of a low-redshift sample of 14 quasars, covering wide rest wavlengths 1000–7300 Å, and claimed that the Fe II strength correlates with the mass of the central black hole, the line width and the X-ray photon index.

In this paper, we present spectra of six quasars at $z \sim 2$ and compare with those in the low-redshift sample. Throughout this paper, a cosmology with $\Omega_m = 0.3$, $\Omega_\Lambda = 0.7$ and $H_0 = 70$ km s^{-1} Mpc^{-1} is assumed.

2 OBSERVATIONS

Six quasars were selected for optical spectroscopy from the catalogue by Véron-Cetty & Véron (2003). According to the catalogue, these are luminous with $M_B = -28$ to -31 at $z = 2.0$–2.3, bright enough to take optical Fe II emission lines through near-infrared spectroscopy at a later opportunity.

Gemini Multi-Object Spectrographs (GMOS) on Gemini South Telescope are used in the long-slit mode with grating R150_G5326 and order sorting filter OG515_G0330. Wavelengths observed are in 5400–9800 Å, corresponding to rest

★E-mail: hsameshima@ioa.s.u-tokyo.ac.jp

Table 1. Observing log for Gemini quasars.

Object	α	δ	Redshift[a]	M_B[b] (mag)	E^c_{B-V} (mag)	Exposure time (s)	Date
B0226−104	02 28 39.2	−10 11 10	2.276	−29.7	0.03	120	2004 September 18
B0421+019	04 24 08.6	+02 04 25	2.059	−27.8	0.19	600	2004 September 18
CTQ254	04 30 14.6	−36 26 47	2.118	−27.7	0.02	1500	2004 September 18
FIRSTJ2149−0811	21 49 48.2	−08 11 16	2.128	−28.9	0.04	150	2004 September 20
LBQS2209−1842	22 12 10.4	−18 27 38	2.093	−27.4	0.03	960	2004 September 20
PHL424	23 13 24.5	+00 34 45	2.087	−28.5	0.04	300	2004 September 21

[a]Redshift as determined from fit of Mg II emission line.
[b]Absolute B magnitude with $\Omega_m = 0.3$, $\Omega_\Lambda = 0.7$ and $H_0 = 70$ km s^{-1} Mpc^{-1}.
[c]Galactic extinction E_{B-V} taken from Schlegel et al. (1998).

wavelengths 1800–3300 Å at $z \sim 2$ quasars. The slit width is 1.0 arcsec and the spectral resolution is 3.286 Å pixel^{-1}. The grating was centred at 8150 Å for the first three exposures and changed to 8250 Å for the following exposures, filling up the gaps of the charge-coupled device (CCD) chip array. Wavelengths were calibrated using the CuAr arc lamp taken at both central wavelengths of the grating. LTT1788 (Hamuy et al. 1994) was used for flux-scaling. The observing log is summarized in Table 1.

Individual spectral frames were processed using the Gemini : IRAF package version1.9.1. Sky of individual frames is subtracted with GSSKYSUB, and then SCOMBINE was used to combine into the final spectral frame. The corrections for telluric absorption were not applied. Reduced spectra are shown in Fig. 1. Redshifts are determined from fit of Mg II emission line. With these measured redshifts, absolute B magnitudes are calculated assuming a cosmology with $\Omega_m = 0.3$, $\Omega_\Lambda = 0.7$ and $H_0 = 70$ km s^{-1} Mpc^{-1}. Redshifts and absolute B magnitudes are also listed in Table 1.

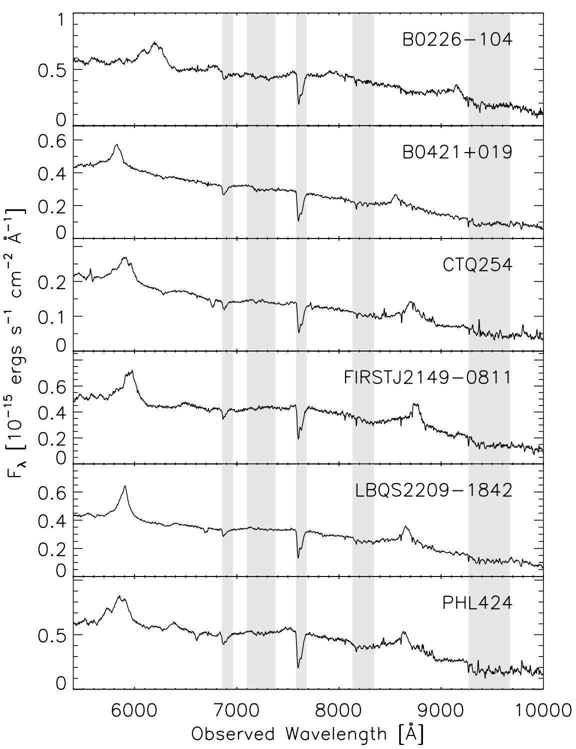

Figure 1. Spectra of six quasars. The shaded area indicates the region where the spectra are affected by the telluric absorption.

3 MEASUREMENT OF EMISSION LINES

Prior to measuring physical quantities such as Fe II emission lines, the quasar spectra were dereddened for the Galactic extinction according to the dust map by Schlegel et al. (1998) using the Milky Way extinction curve by Pei et al. (1992). E_{B-V} of the Galactic extinction is listed in Table 1. In the shaded area in Fig. 1, the telluric absorption features are seen. We have not applied any correction for the telluric absorption. Instead, the intensities in the shaded areas were estimated by fitting a linear function to assumed data points located on either side free from the telluric features.

3.1 Fe II UV emission lines

Fe II emission lines are heavily blended with each other, forming the broad features from 2000 to 3000 Å. It is desirable to observe a wide range of wavelengths in such a way that the power law and Balmer continua are accurately determined as made by Tsuzuki et al. (2006). However, observing such a wide range is not feasible in most cases. In fact, the present observations are limited to a rest wavelength range from 1600 to 3200 Å.

We applied a simple alternative in which a linear function is fit to the data in rest wavelengths 2190–2230 and 2660–2700 Å. Differences between the spectrum and the resultant best-fit function, which are marked as shade in Fig. 2, are summed up in a wavelengh range of 2240–2650 Å. The summed-up differences, as denoted by f(2240–2650 Å), should contribute significant part of Fe II (2000–3000 Å) which is the *total* Fe II emission line flux in 2000–3000 Å. To check the relationship between them, we have applied this alternative to the low-redshift quasars studied by Tsuzuki et al. (2006) for which Fe II (2000–3000 Å) is known. The results are shown in Fig. 3(a). This figure indicates that the relation is linear and f(2240–2650 Å) is approximately 40 per cent of Fe II (2000–3000 Å). A least-squares fitting to the data gives the following relation:

$$\log \mathrm{Fe\,II} = \log f + 0.402(\pm 0.142). \qquad (1)$$

Here, Fe II ≡ Fe II (2000–3000 Å) and $f \equiv f$(2240–2650 Å).

This relation will be used to convert observed f(2240–2650 Å) to the total flux of the Fe II emission lines in 2000–3000 Å in the later part of this paper.

3.2 Mg II emission lines

To measure the flux and the full width at half maximum (FWHM) of the Mg II λ2798 doublet, Tsuzuki et al. (2006) fitted a single Gaussian component to the spectrum where the power law and Balmer continua and Fe II emission features were already subtracted.

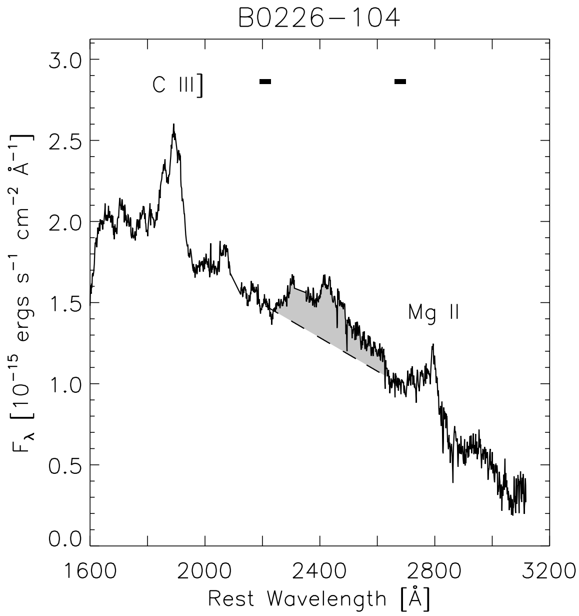

Figure 2. Measuring the UV Fe II line flux. A linear function is fit to the data in the continuum windows (thick bars). The best-fit function is indicated by the dashed line. The shaded area indicate f(2240–2650 Å), which is then converted to Fe II (2000–3000 Å) using equation (1).

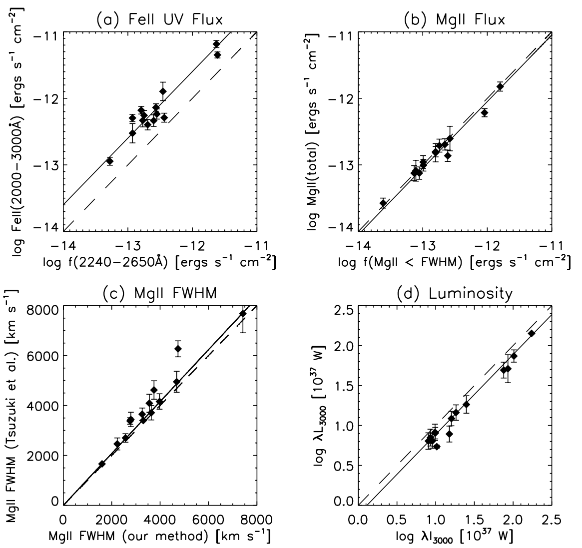

Figure 3. Comparison of the physical quantities in the low-redshift sample measured between the two methods; data along the horizontal-axis are measured by our method and those along the vertical-axis by Tsuzuki et al. (2006). The dashed line indicate $y = x$ where two measurements result in the identical values, and the solid line indicates the best-fit line. Each panel shows (a) Fe II(2000–3000 Å) [erg s^{-1} cm^{-2}], (b) Mg II(*total*) [ergs s^{-1} cm^{-2}], (c) FWHM(Mg II) [km s^{-1}] and (d) 3000 Å Luminosity [10^{37} W].

Again, we are not allowed to apply their method because of our limited wavelength range.

Our alternative is illustrated in Fig. 4. A linear function is fit to the data in 2660–2700 and 2930–2970 Å where contributions from the Fe II and Mg II emission lines are relatively weak and

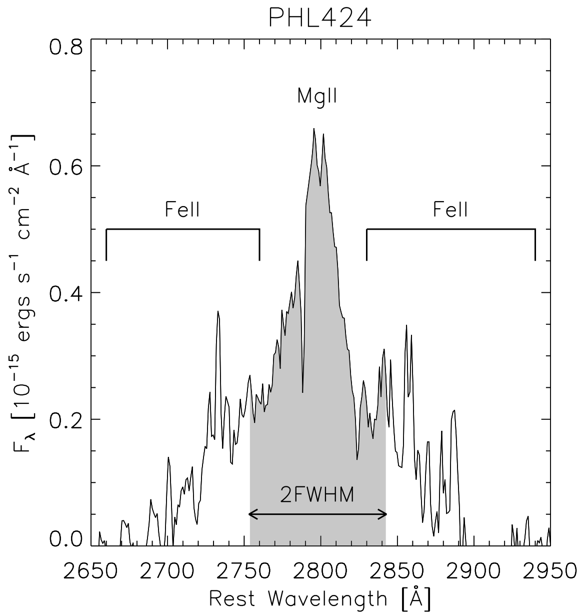

Figure 4. Measuring the Mg II flux. Since there are Fe II emissions underneath Mg II, we measured the flux only over the velocity range −FWHM < v(Mg II) < FWHM and defined it as f(Mg II < FWHM) (shaded area).

thus the power-law continuum can be defined.[1] This fitted function is subtracted from the spectrum, as shown in Fig. 4. To measure the Mg II FWHM, we first applied smoothing to that subtracted spectrum, then measured the velocity range within which the flux becomes more than half of its maximum value and defined it as FWHM. To minimize contributions from Fe II emission, we only integrate the flux within −FWHM < v(Mg II) < FWHM and define it as f(Mg II < FWHM). Again, we used the low-redshift sample by Tsuzuki et al. (2006) to check that the relation between f(Mg II < FWHM) and the *total* Mg II flux Mg II(*total*). The results are shown in Figs 3(b) and (c). f(Mg II < FWHM) has linear relation to the *total* Mg II line flux measured by Tsuzuki et al. (2006), and the least-squares best-fit to the data gives the following relation:

$$\log \mathrm{Mg\,II}(total) = \log f(\mathrm{Mg\,II} < \mathrm{FWHM}) - 0.049(\pm 0.084). \quad (2)$$

This will be used to obtain Mg II(*total*) in the later part of this paper. It is noted that there are no significant differences in FWHM of Mg II between the measurements by Tsuzuki et al. (2006) and our alternative.

3.3 Luminosity

McLure & Jarvis (2002) gives a method for estimating black hole masses of quasars using the FWHM of the Mg II emission line and the continuum luminosity at 3000 Å. The equation is as follows:

$$\frac{M_{\rm BH}}{\rm M_{\odot}} = 3.37 \left(\frac{\lambda L_{3000}}{10^{37}\rm W}\right)^{0.47} \left[\frac{\rm FWHM(Mg\,II)}{\rm km\,s^{-1}}\right]^{2}. \quad (3)$$

Note that the uncertainty of equation (3) is a factor of 2.5.

Hence, the monochromatic luminosity λL_{3000} has to be measured in order to estimate the black hole mass. Unfortunately, however, our spectra are significantly affected by telluric absorption at 3000 Å. We thus extrapolated the linear function, which was used to measure

[1] 3000–3050 Å would be a better choice than 2930–2970 Å, if the CCD fringe pattern can well be removed in these wavelenghts.

Table 2. Measured physical quantities.

Object	Fe II (2000–3000 Å)[a] (10^{-14} erg s^{-1} cm^{-2})	Mg II(*total*) (10^{-14} erg s^{-1} cm^{-2})	FWHM(Mg II)[b] (km s^{-1})	λL_{3000} (10^{37} W)	$M_{\rm BH}$ (10^9 M$_\odot$)
B0226−104	19.3 (+7.5/−5.4)	–	—	—	–
B0421+019	5.46 (+2.1/−1.5)	1.24 (+0.26/−0.22)	4410 (+520/−470)	369 (+74/−62)	1.05 ± 0.269
CTQ254	3.11 (+1.2/−0.87)	0.726 (+0.16/−0.13)	4750 (+570/−510)	161 (+32/−27)	0.828 ± 0.212
FIRSTJ2149−0811	14.1 (+5.5/−3.9)	2.16 (+0.46/−0.38)	3900 (+460/−410)	500 (+100/−83)	0.951 ± 0.243
LBQS2209−1842	8.78 (+3.4/−2.5)	1.70 (+0.36/−0.30)	4180 (+500/−440)	360 (+72/−60)	0.935 ± 0.239
PHL424	19.5 (+7.6/−5.5)	2.81 (+0.60/−0.49)	5000 (+590/−530)	587 (+120/−98)	1.69 ± 0.431

[a]Fe II is defined in a wavelength range of 2000–3000 Å.
[b]FWHM of the Mg II emission line.

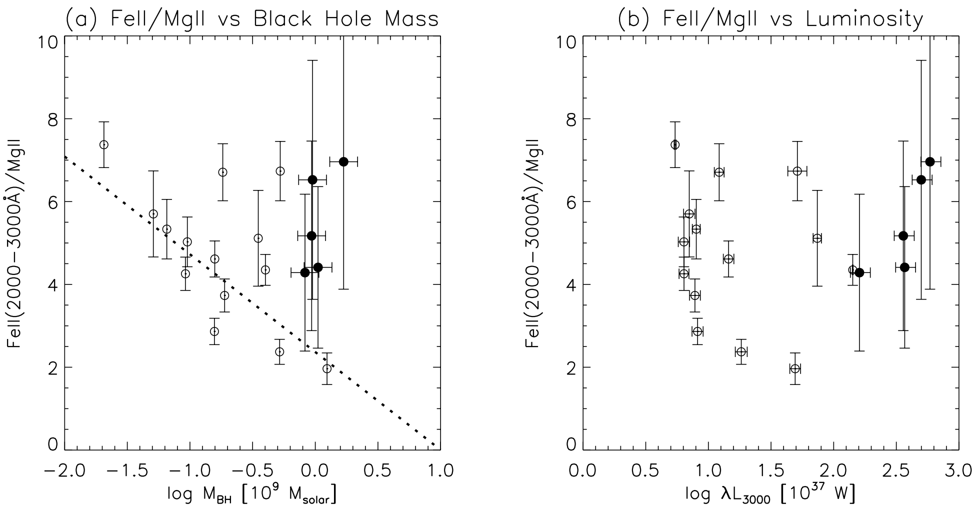

Figure 5. (a) Relation between Fe II(UV)/Mg II flux ratio and black hole mass. Filled circles are our quasars at $z \sim 2.0$. Open circles are low-redshift quasars at $z = 0.06$–0.55 by Tsuzuki et al. (2006). Dotted line indicates the correlation found in Tsuzuki et al. (2006). (b) Same as in (a), but for 3000 Å luminosity.

f(Mg II < FWHM), to 3000 Å and read the value at 3000 Å as a monochromatic flux. Fig. 3(d) compares the 3000 Å luminosity λL_{3000} measured by Tsuzuki et al. (2006) and our extrapolated 3000 Å luminosity λl_{3000}. Again, the linear relation was obtained as follows:

$$\log \lambda L_{3000} = \log \lambda l_{3000} - 0.112(\pm 0.079). \quad (4)$$

This will be used to convert extrapolated luminosities to the real luminosity in the later part of this paper.

4 RESULTS

In Table 2, the Fe II emission line flux Fe II (2000–3000 Å), the Mg II line flux Mg II(*total*), the FWHM (Mg II), the 3000 Å luminosity λL_{3000} and the black hole mass $M_{\rm BH}$ derived from equation (3) are given. Note that, for B0226−104, Mg II emission line is heavily affected by telluric absorption line, so that we did not measure Mg II flux and Mg II FWHM. A plot of Fe II (2000–3000 Å)/Mg II(*total*) against $M_{\rm BH}$ is given in Fig. 5(a) and 3000 Å luminosity λL_{3000} in Fig. 5(b).

5 DISCUSSION

Analysing 14 low-redshift quasars, Tsuzuki et al. (2006) found the correlation between the flux ratio Fe II(UV)/Mg II and the black hole mass. This relation is shown by the dotted line in Fig. 5(a). Filled circles are our quasars at $z \sim 2.0$ and open circles are low-redshift quasars at $z = 0.06$–0.55 by Tsuzuki et al. (2006). Our quasars have an absolute luminosity of $M_{\rm B} < -27.4$, which are much luminous than the low-redshift quasars having an absolute luminosity of $M_{\rm B} > -26.3$.

As can be seen in Fig. 5(a), the five $z \sim 2$ quasars do not follow the correlation found by Tsuzuki et al. (2006). All of them have Fe II(UV)/Mg II greater than expected from the Tsuzuki's correlation. What is the cause of the large Fe II(UV)/Mg II value in the $z \sim 2$ quasars relative to the low-redshift quasars? Because the five $z \sim 2$ quasars are much luminous than the 14 low-redshift quasars, the luminosity effect is examined. As shown in Fig. 5(b), the luminosity effect is not responsible for the large Fe II(UV)/Mg II value in the $z \sim 2$ quasars. The *real* cause would be evolution in Fe II(UV)/Mg II or non-abundance effects such as the spectral energy distribution of the continuum from the central source, the strength of the radiation field and the gas density of BELR clouds as well as the microturbulence of BELR gas (Verner et al. 2003; Baldwin et al. 2004). Further investigations are required using large samples of quasars.

ACKNOWLEDGMENTS

This work was financially supported in part by Grant-in-Aid for Scientific Research (17104002) and Specially Promoted Research (20001003) and the Japan–Australia Research Cooperative Program from JSPS.

REFERENCES

Baldwin J. A., Ferland G. J., Korista K. T., Hamann F., LaCluyzé A., 2004, ApJ, 615, 610
Dietrich M., Appenzeller I., Vestergaard M., Wagner S. J., 2002, ApJ, 564, 581
Dietrich M., Hamann F., Appenzeller I., Vestergaard M., 2003, ApJ, 596, 817
Elston R., Thompson K. L., Hill G. J., 1994, Nat., 367, 250
Freudling W., Corbin M. R., Korista K. T., 2003, ApJ, 587, L67
Friaça A. C. S., Terlevich R. J., 1998, MNRAS, 298, 399
Granato G. L., De Zotti G., Silva L., Bressan A., Danese L., 2004, ApJ, 600, 580
Hamann F., Ferland G., 1993, ApJ, 418, 11
Hamuy M., Suntzeff N. B., Heathcote S. R., Walker A. R., Gigoux P., Phillips M. M., 1994, PASP, 106, 566
Iwamuro F., Motohara K., Maihara T., Kimura M., Yoshii Y., Doi M., 2002, ApJ, 565, 63
Iwamuro F., Kimura M., Eto S., Maihara T., Motohara K., Yoshii Y., Doi M., 2004, ApJ, 614, 69
Kawara K., Murayama T., Taniguchi Y., Arimoto N., 1996, ApJ, 470, L85
Kurk J. D. et al., 2007, ApJ, 669, 32
Maiolino R., Juarez Y., Mujica R., Nagar N. M., Oliva E., 2003, ApJ, 596, L155
Matsuoka Y., Oyabu S., Tsuzuki Y., Kawara K., 2007, ApJ, 663, 781
Matsuoka Y., Kawara K., Oyabu S., 2008, ApJ, 673, 62
Matteucci F., Recchi S., 2001, ApJ, 558, 351
McLure R. J., Jarvis M. J., 2002, MNRAS, 337, 109
Pei Y. C., 1992, ApJ, 395, 130
Schlegel D. J., Finkbeiner D. P., Davis M., 1998, ApJ, 500, 525
Tsuzuki Y., Kawara K., Yoshii Y., Oyabu S., Tanabé T., Matsuoka Y., 2006, ApJ, 650, 57
Verner E., Bruhweiler F., Verner D., Johansson S., Gull T., 2003, ApJ, 592, L59
Véron-Cetty M.-P., Véron P., 2003, A&A, 412, 399
Yoshii Y., Tsujimoto T., Kawara K., 1998, ApJ, 507, L113
Yoshii Y., Tsujimoto T., Nomoto K., 1996, ApJ, 462, 266

This paper has been typeset from a TEX/LATEX file prepared by the author.